

Heat Treatment of NIST T-200 CVN Specimens

Introduction

A T-type maraging steel was used to produce very-high-energy (near 200 J) verification specimens that are tested to certify the performance of Charpy impact test machines. The steel is an 18 % nickel alloy in which titanium (rather than cobalt) is used as the primary strengthening element. In a peak aged condition, these alloys would be expected to have Charpy impact energies of around 110 J (80 ft-lbs) and hardness of about 43 to 47 HRC (Rockwell C scale). NIST uses the alloy to produce specimens with much higher impact energy, however, and refers to these specimens as superhigh-energy specimens. Our super high energy verification specimens have impact energies typically in the range of 175 to 245 J (130 to 180 ft-lbs).

We recently purchased a new heat of T-type maraging steel and planned a study to help optimize the heat treatment for this new steel and reduce the variation in impact energy of the specimens. Issues of primary interest to this study include: (1) redistribution of indigenous inclusions by solution heat treatment, to evaluate the effect on the fracture energy and scatter in impact energy; (2) grain refinement and beneficial effects of multiple recrystallizations on the variation in absorbed energy; (3) grain size and morphology effects, and (4) controlled cooling and its effect on the degree of embrittlement and impact toughness.

Literature Review

There has been a significant amount of research done on T-type maraging steels, but there is still disagreement on several of the factors that interest us. It is beyond our scope to present a full literature review here, but a number of the pertinent papers are discussed and referenced in the following review.

Transformation in Maraging Steels

The phase transformations that are of the most interest for the 18 % Ni maraging steels are the martensite transformation on cooling and the formation of austenite on heating (holding at temperature). As shown in **Figure 1**, martensite is quite stable during heating, which makes possible the aging of the martensite. Data cited for T-250 Maraging steels in **Table 1**, gives A_s and A_f temperature bounds for the $\alpha+\gamma$ region of 661 °C and 730 °C (1223 and 1346 °F), respectively.^{1,2,3} However, substantial amounts of reverted austenite can form in Co-free maraging steels (and other maraging steels) during aging treatments at temperatures of less than the A_s temperature.

Table 1: Transformation temperature (reported in Sarma paper, from references)

Steel	M _s C(F)	M _f C(F)	A _s C(F)	A _f C(F)
T-250 Co-free	253 (487)	115 (239)	662 (1223)	730 (1346)
M-250 7.8 Co	209 (410)	90 (194)	630 (1166)	720 (1328)

There are several ways to introduce austenite into the microstructure of martensitic steels: (1) isothermal heating in the two phase austenite + ferrite region, where austenite nucleates and grows (at Ni-rich precipitates and lath boundaries), and (2) thermal cycling at predetermined heating and cooling rates between the single phase austenite region and room temperature, which results in enriched austenite that does not transform to martensite on cooling. In the first case, the austenite is referred to as reverted austenite, in the second as retained austenite. The nickel-enriched austenite has been reported to be stable down to $-415\text{ }^{\circ}\text{F}$ (77 K), and is suspected of having high chemical inhomogeneity. In addition, austenite appears to be hardened by high dislocation densities that result from phase work hardening (due to an apparent α -martensite $\rightarrow \gamma$ cooperative transformation mechanism that has some similarities to a martensitic transformation).

It is not clear whether reverted or retained austenite adversely affect the scatter in CVN energy. Some authors report no effect of the stable austenite on the impact toughness, but some others report beneficial effects. The effects are likely to be unlike those for retained austenite in other carbon and alloy steels.

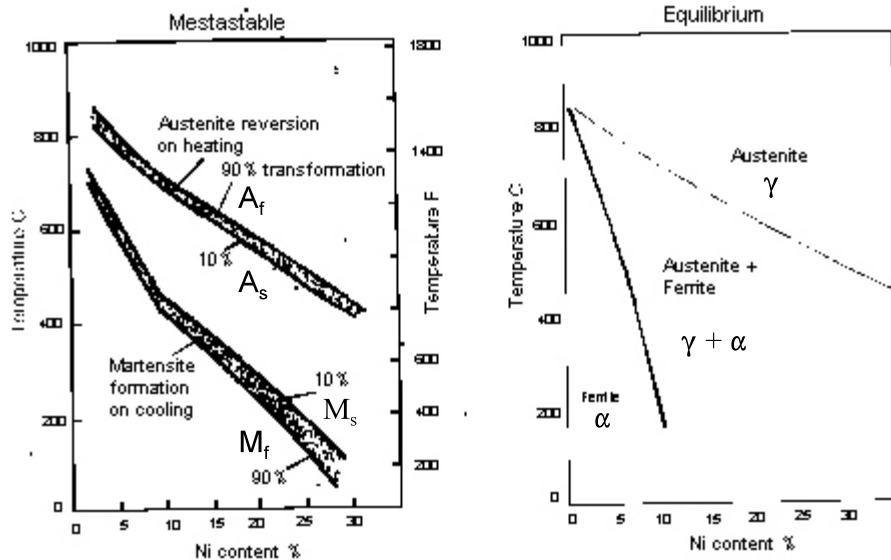


Figure 1. Metastable and equilibrium phase relationship in the Fe-Ni system. These diagrams are based on those shown for maraging steels in the Metals Handbook, Desk Edition, (ASM Metals Park, Ohio), p. 4-57.

Studies of temperature cycling by Viswanathan show that maraging steels are sensitive to rates of heating and cooling.⁴ This study used a steel that was solution-annealed at 950 °C (1750 °F) for two hours, air-cooled, then annealed at 820 °C (1500 °F) for 3.5 hours and air-cooled. The steel was then either conventionally aged at 510 °C (950 °F) for 3 hours or thermally cycled and water quenched. Thermal cycling was done at 6 °C per min or 9.5 °C per min or 11.5 °C per min. Cycling was between room temperature and A_f (determined to be 1400 °F; at a heating rate of 750 °C). The retained austenite was found to increase with the number of cycles. The faster cycling rate produced more retained austenite (66 % after five cycles, but at 9.5 °C/min, a single cycle produced about 40 %). The cycling produces solute-rich austenite that does not transform on cooling and this results in a less saturated martensitic phase, which reduces the precipitate strengthening. The Charpy V-notch toughness increased from 12 to 70 J (0 to 60 % Aus) for specimens in the aged condition as the amount of austenite went from 0 to 60 %.

Grain size and morphology

Work by Sinha on a Co-free (250 grade) maraging steel showed the effect of grain size on toughness.⁵ The steel had a composition of 0.008 C, 17.1 Ni, 2.25 Mo, 1.39 Ti, 0.01 Al, 0.01 S, 0.008 P, 0.004 O₂, and 0.003 N₂. In the study, hot-rolled pieces were solution-annealed at 7 different temperatures for 1 h (air-cooled) and evaluated for microstructure, strength, impact toughness and fracture toughness. Some of the specimens were aged at 477 °C (890 °F) and some were tested in the unaged condition. Full recrystallization occurred after holding for an hour at 825 °C (1520 °F), and this treatment resulted in the optimum strength/toughness combination (full ductile dimple rupture, no ridges, 25 µm blocky martensite). Grain growth occurred at temperatures above 852 °C (1565 °F), accompanied by a gradual change in the martensite lath morphology from blocky to stringer type. The transformation corresponded to a grain size of 35-40 µm. The transformation to stringer type was complete at 1052 °C (1925 °F). Interestingly, this transformation was correlated to a reduction in tensile ductility, fracture toughness, and CVN. There was another decrease in toughness for the 1052 °C (1925 °F) specimens that was attributed to precipitation at grain boundaries. The CVN energy was the least changed of the toughness indicators measured, and was most constant for specimens annealed between the temperatures of 850 and 1000 °C (1565 and 1835 °F). All the CVN data, however, were for aged specimens. (It was also determined in the Sinha study that grain size has little effect on strength, because the martensite lath spacing was not changed by change in grain size.)

Another study by Sinha (T-250 Co-free and M-250 7.5 Co) detailed grain-growth behavior for maraging steel.⁶ In this study, isothermal annealing temperatures were used: the specimens were initially annealed for 1 h at 825 °C (1520 °F) and air cooled, then held for times of 0.25 to 10 h at temperatures ranging from 900 to 1050 °C (1655 to 1925 °F). The results show that only modest grain growth (less than 50 µm) occurred for the T-250 Co-free steel at 900 °C (1655 °F) for times up to 3 h. Longer holding times, even at these low temperatures, were shown to sometimes result in abnormal grain growth.

It seems to be generally recognized that grain refinements can be attained in maraging steels by cyclic heating and cooling treatments. Specimens with large grain sizes (hundreds of

micrometers) can be refined to some minimum size (less than 50 micrometers), after which cyclic treatments do not result in further refinement. The paper by Saul addresses this issue for the 250 and 300 grade maraging steels.¹ However, no paper we reviewed presented clear evidence of how and why the refinement occurs, or why the particular treatment schedule is apparently so dependent on the specific composition (or initial microstructure) of the steel.

Aging

Most research does not include aging data for temperatures as low as those used to produce NIST T-200 impact verification specimens (315 °C), because aging temperatures this low are not of commercial interest. There has been some indication, however, that aging at low temperatures results in the formation of precipitates different from those typical of the 480 °C (900 °F) aging treatment that is commonly used for these alloys.

Studies on an 18 Ni Co-containing 350 grade maraging steel and on T-250 Co-free maraging steel showed differences in the precipitates formed above and below 450 °C (845 °F).^{7,8} The studies indicate that Ni₃Ti precipitates are formed in the alloys at high aging temperatures, but at low aging temperatures (315 °C, 3 h) actual precipitation probably does not occur. It is more likely that clusters of Ni and Ti atoms cause the strengthening. The study by Sinha, which includes aging temperatures as low as 468 °C on T-250 Co-free maraging steel, shows that the hardening due to aging was rapid (increases of 80 to 90 % within the first 15 to 30 min). Interestingly, the toughness of the under-aged maraging steels in the Sinha study was lower than the toughness for the peak-aged steels. This is apparently due to the clusters or coherent precipitates that are present in the under-aged condition, which restrict cross slip in the matrix. In the peak-aged condition, precipitates (Ni₃Ti) are formed that allow more homogeneous slip in the matrix.

Thermal embrittlement

Maraging steel can become embrittled during high-temperature solution-annealing treatments. The embrittlement is caused by precipitation of Ti (C, N) at grain boundaries during cooling, and can be retained even following re-annealing. Quenching from high temperature prevents the precipitation and subsequent embrittlement.

Sinha studied thermal embrittlement in a T-250 maraging steel and showed that marked degradation in toughness can result when the steel is cooled from high temperature and held between 785 and 400 °C (1450 and 1750 °F).⁹ In the study, two heat treatments were used: (1) HT1, solution-treated at 1200 °C (2192 °F) for 1 h and quenched to intermediate temperature for a hold of 180 min then air-cooled, (2) HT2, solution-treated at 1200 °C (2192 °F) and water quenched, then reheated to intermediate temperature for 180 min and air cooled. The composition of the T250 steel used in the study was 0.006 C, 0.005 P, 0.001 S, 2.25 Mo, 17.1 Ni, 0.10 Al, 0.003 N, 1.39 Ti, and 0.004 O. The steels were tested in unaged and aged conditions (aged at 480 °C for 3 h). The impact energy of the HT1 as-quenched steel was 188 J, compared to 25 J for the HT1 specimens that were held at intermediate temperatures and embrittled. No effect of embrittlement was found at any intermediate temperature for the HT2 treatment (about 190 J for

all intermediate treatments). So embrittlement occurred only when the steel was directly cooled to an intermediate holding temperature.

Other embrittlement studies have shown that the steel must be quenched from re-annealing treatments to avoid embrittlement, but Sinha reasons that in his study there was uniform precipitation of Ti (C,N) on the dislocations formed during the transformation to austenite on the reheating of the solution-annealed and quenched steel (and this kept the Ti out of solution, where it could not segregate to grain boundaries during cooling from the re-annealing treatment).

Inclusions

One would hope that a solution-treatment could be used, in concert with controlled heating and cooling to dissolve and redistribute the large Ti(N,C) inclusions in the T-type maraging steels. This matter is of practical interest because these inclusions can have a significant effect on the homogeneity of the initiation and propagation of ductile tearing in the steel. The solution treatment could also help to redistribute chemical inhomogeneity in the material that might reduce variation in impact properties.

Summary of Past Heat Treatments on the NIST T-200 Bar Stock

A number of heat treatments have been done on the T-200 material at NIST and by NIST contractors. Results from these heat treatments have contributed to our general understanding of this particular heat of T-200 steel, and we discuss some specific details below.

Initial heat treatments on the T-200 material provided a general understanding of the energy levels that might be expected. The mechanical test results for two of the heat treatments are shown in **Figures 2-4**. In **Figures 2 and 3**, the specimens were annealed at 955 °C (1750 °F) for 1 h and air-cooled, then re-annealed at 760 °C (1400 °F) for 1 h and air cool. These specimens were then divided into five groups and aged at 260 °C (500 °F), 288 °C (550 °F), 315 °C (600 °F), 343 °C (650 °F), and 370 °C (700 °F) for 3 h and air-cooled. The data show the relationship between the impact energy and the hardness of the specimens, and indicate that specimens aged at less than 300 °C can reach toughness levels near 200 J.

The data in **Figure 4** are similar to that in **Figure 2**, but these specimens were annealed at 900 °C (1650 °F) for 1 h and water-quenched, then reheated twice to 675 °C (1250 °F) and water-quenched as a grain refinement treatment, and re-annealed at 815 °C (1500 °F) for 1 h and air-cooled prior to aging at 315 °C (600 °F) and then at 370 °C (700 °F) for 3 h. Other variations

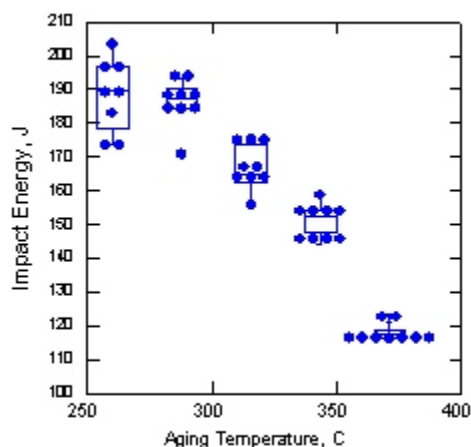


Figure 2: Impact energy versus aging temperature.

of these two heat-treatment schedules produced similar results. Overall, it appears that this T-200 material can be annealed and aged to produce Charpy specimens having impact energies of 200 J. The hardness of specimens with impact energies of 115 to 205 J ranged from 40 to 32 HRC.

As shown in **Figure 5**, quenching from the annealing temperature clearly results in a softer (tougher) material, and the difference in hardness is retained after aging (compared with air-cooled). These data are from specimens heat-treated at NIST in laboratory furnaces. The specimens were produced mainly for microstructure evaluations, but hardness tests were made to give some indication of the toughness. We found a difference of about 5 HRC, between the quenched and unquenched specimens, which may be helpful in increasing the toughness of the lots. Based on the results shown in **Figures 2 and 3**, an increase in toughness on the order of 30 or 40 J might be associated with a difference in hardness of 5 HRC.

Microstructural evaluations on laboratory specimens suggested limits on annealing temperatures to control grain growth, treatments to refine the grain size, and procedures to control retained austenite levels in the specimens. Examples of the microstructures observed for the specimens are given in **Figure 6-13**.

The as-received T-200 bar stock (**Figure 6**) has a small grain size (likely 10 μm or less), which is desirable. The grain boundaries are decorated with particles or retained austenite. Based on microstructural observations of the specimens heat-treated in our laboratory furnace, grain refinement is attainable. For example, the microstructure shown in **Figure 7**, which has a grain size of about 25 μm or so, was produced from a microstructure having an initial grain size of about 50 μm . In this case, the grain refinement was attained by slowly cooling the specimen through the two-phase region (to room temperature), then reheating and holding it at the temperature where reverted austenite forms, prior to re-annealing the specimen.

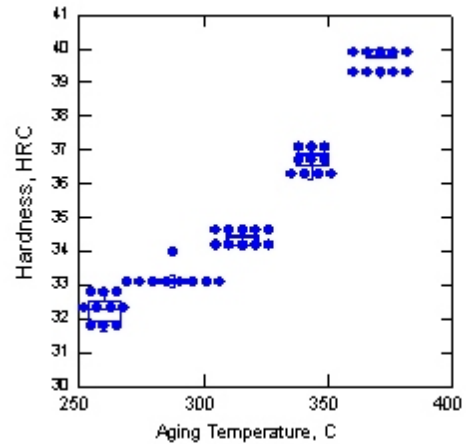


Figure 3: Hardness distributions.

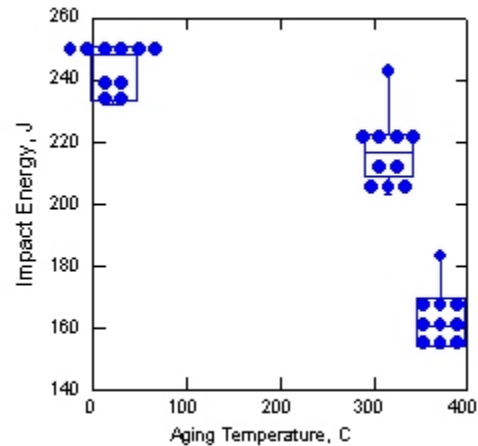


Figure 4: Absorbed energy distributions.

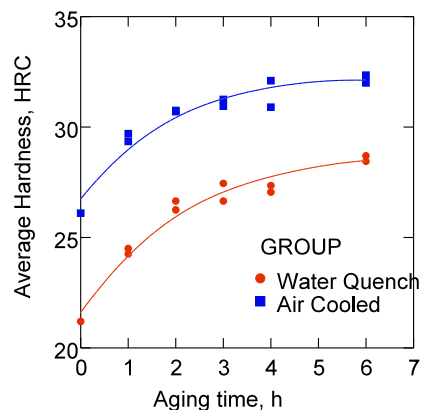


Figure 5: Average hardness trends.

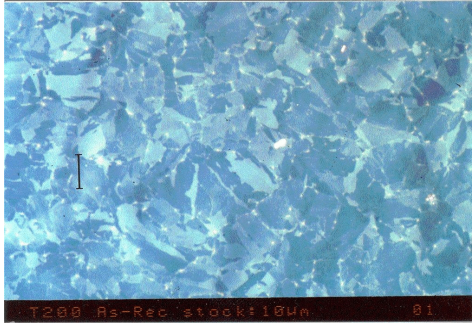


Figure 6. Microstructure of the as-received T-200 bar stock. Bar equal to 10 μm .



Figure 7. Specimen was annealed at 870 $^{\circ}\text{C}$ air-cooled, re-heated to 575 $^{\circ}\text{C}$ and air cooled, then re-annealed at 840 $^{\circ}\text{C}$ and air-cooled. Bar is equal to 20 μm .

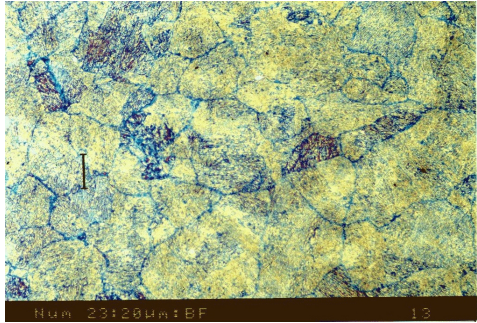


Figure 8. Specimen was annealed at 870 $^{\circ}\text{C}$ and air-cooled, then re-heated to 660 $^{\circ}\text{C}$ for 1 h and water-quenched. Bar equal to 20 μm .

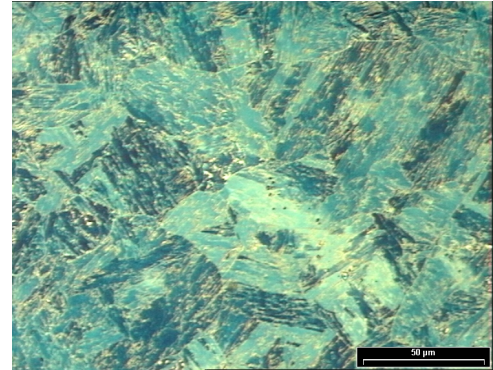


Figure 9. Specimen was annealed at 890 $^{\circ}\text{C}$ and water quenched, then re-heated to 590 $^{\circ}\text{C}$ for 1 h and water-quenched. Bar equal to 50 μm .

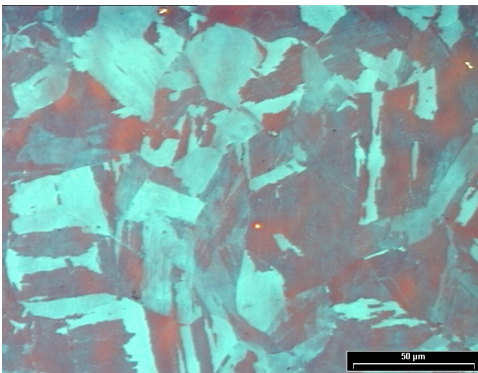


Figure 10. Specimen annealed at 890 $^{\circ}\text{C}$ and water-quenched. Bar equal to 50 μm .

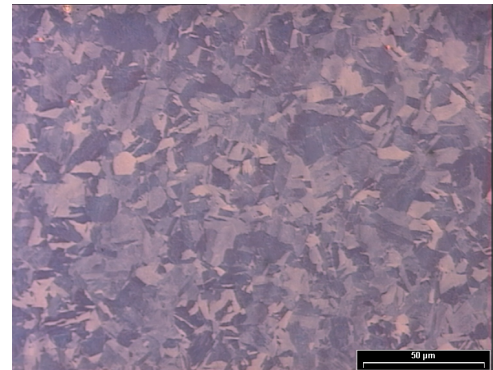


Figure 11. Specimen was heated to 600 $^{\circ}\text{C}$ for 1 h, water-quenched, then reheated to 660 $^{\circ}\text{C}$ for 30 min, then to 840 $^{\circ}\text{C}$ and held 1 h and water-quenched. Bar equal to 50 μm .

In **Figures 8 and 9**, results of holding the specimens at temperatures below the A_f temperature are shown. In **Figure 8**, the microstructure of the specimen, which was held in the two-phase $\alpha + \gamma$ region, has clearly delineated austenite grain boundaries. The basic morphology of the grains has changed to an equiaxed austenite-like morphology. However, the grains contain a fine two-phase structure of reverted austenite and α -martensite, and occasional regions of a coarser two-phase structure. In **Figure 9**, the microstructure of the specimen, which was held at a temperature just below the two-phase region, has significant amounts of reverted austenite at prior austenite grain boundaries and between laths of martensite within the grains.

We did not determine the A_s or the A_f temperature in our experiments, but the estimates given by Sarma in **Table 1** appear to be reasonable for our T-200 material. Our observations also indicate that specimens containing reverted austenite could not be fully annealed when treated at 760 °C (1400 °F) with holding times of 1 h. So, we might consider 815 °C (1500 °F) to be a minimum temperature for annealing treatments. A maximum annealing temperature of about 870 °C (1600 °F) is suggested by our testing, because we see significant grain growth for annealing treatments done at 925 °C (1700 °F) for 1 h, and some grain growth likely also occurred for the 890 °C (1650 °F) annealing treatments, as indicated by the microstructure shown in **Figure 10**.

Overall, the laboratory heat-treatment experiments showed that temperature cycling between room temperature and the two-phase region (and below A_s) yielded some grain refinement in our T-200 material. However, cycles between room temperature to slightly above A_f also yielded some grain refinement, and this cycle avoids the formation of too much reverted austenite. We found that when grain growth occurred due to annealing or solution treatments, it was possible with additional heat treatments to refine the grain size with additional heat treatments back to a reasonably small size (25 μm).

The final topic of discussion here is the grain morphology, because there are two characteristic grain morphologies typical of the specimens. Grain morphologies with little grain-boundary definition (like shown in **Figure 10**) and a resolvable stringer-type martensite (not shown) occur in specimens annealed at higher temperatures. The literature indicates that the morphology is a function of grain size, where the morphology changes at grain sizes near 35 or 40 μm . At smaller grain sizes, the specimens tend to have grain morphologies more like those shown in **Figure 11**. Here, the grain boundaries were etched to mark and delineate the grain boundaries, and the martensite morphology is blocky (according to Sinha) which likely results in the different appearance of the grains. Our T-200 verification specimens that have had the lowest variations in impact energy have had this small grain morphology with well delineated grain boundaries.

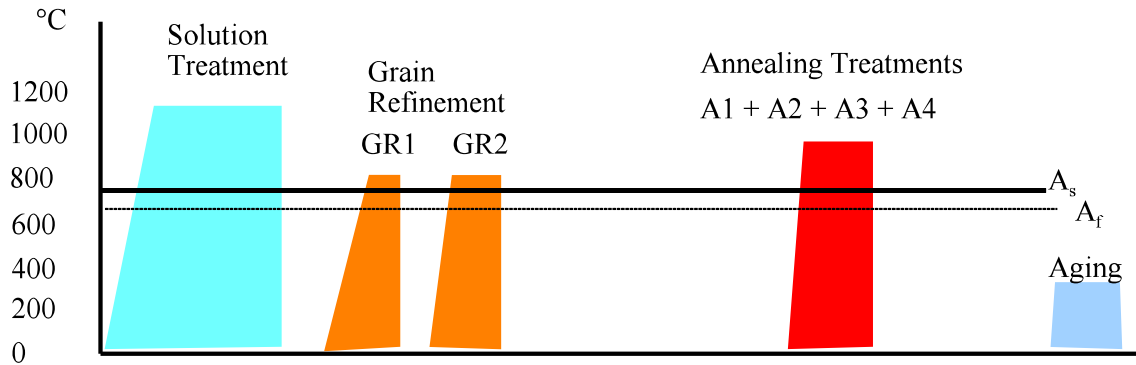


Figure 12: Heat treatment sequence used with reference to the A_s and A_f temperatures.

Materials and Heat Treatments

Three groups of Charpy V-notch specimens were heat-treated by a commercial shop for this study. There were approximately 70 specimens in each group. As shown in **Figure 12** and **Table 2**, the initial heat treatment for the group 1 specimens was as follows: (1) solution treated at 1204 °C (2200 °F) for 1 h and cooled using a 10 bar helium quench, and (2) grain-refinement treatment consisting of a short anneal (GR1) at 815 °C (1500 °F) with a 10 min hold and a 10 bar helium quench, followed by a second anneal (GR2) at 815 °C (1500 °F) for 30 minutes with a 10 bar helium quench. The group 2 specimens did not receive the solution treatment, but did receive the grain refinement treatments (GR1 and GR2). The group 3 specimens received neither the solution treatment nor the grain refinement treatments. So the test matrix has three main legs: (1) group 1, which received a full solution treatment and then grain-refinement steps prior to re-annealing, (2) group 2, which received the same grain refinement steps as the G1 specimens but no solution treatment, and (3) group 3, which was a simple annealing schedule using the as-received material.

Table 2. Heat treatments for the three groups of 1, 2, and 3 specimens. The five specimens taken for evaluation and plotted in Figure 13 are identified.

Group1	Group2	Group3
1204° C ,1 h 10 bar He Specimen 1		
GR1 treatment, 815° C , 10 min, 10 bar He Specimen 2	GR1 treatment, 815° C , 10 min, 10 bar He Specimen 4	
GR2 treatment, 815° C , 30 min, 10 bar He Specimen 3	GR2 treatment, 815° C , 30 min, 10 bar He Specimen 5	
Final anneals (4 variations)	Final anneals (4 variations)	Final anneals (4 variations)
Aging	Aging	Aging

Subgroups of groups 1, 2, and 3, containing 15 to 20 specimens each, were annealed together in the same basket. The four annealing practices were as follows: (1) 830 °C (1525 °F) for 2 h

with a 5 bar helium quench, (2) 830 °C (1525 °F) for 2 h with a 1 bar nitrogen quench, (3) 900 °C (1650 °F) for 2 h with a 5 bar helium quench, and (4) 900 °C (1650 °F) for 2 h with a 1 bar nitrogen quench.

The effect of aging time and temperature on the impact toughness of the specimens was not evaluated. All of the specimens from groups 1, 2, and 3 were aged together at 600 °F for 3 h and quenched in nitrogen at 6 bar.

Specimens for mechanical testing and microstructural evaluations were removed from the group 1 and 2 specimens prior to annealing and aging of the specimens. One specimen was removed from the group 1 specimens following the solution treatment. Another group 1 specimen was removed following the GR1 grain-refinement treatment and still another following the GR2 grain-refinement step. Similarly, two group 2 specimens were removed following the GR1 and GR2 grain-refinement steps, respectively.

Results and Discussion

Solution Treatments and Grain Refinement

The results for the initial heat treatments of the group 1, 2, and 3 specimens indicate that the solution treatment of the T-200 did not result in significantly increased toughness for the material. As shown in **Tables 1 and 2**, and in **Figure 13**, the solution-treated G1 specimen, and the solution-treated and grain-refined G1 specimens had respective impact energies of 224 and 237 J. The G2 specimen, which was not solution treated, had an absorbed energy of 240 J following the grain-refinement treatment. These results are from single specimens, but comparing the solution-treated and grain-refined specimen to the as-received and grain-refined specimen, little difference in the level of toughness is apparent. This implies that the as-received material is a relatively homogenous bulk material and solution treatments might be expected to have only limited effect on the toughness level of the specimens.

The microstructure of the group 1 specimen (**Figure 14**) that was evaluated following the solution treatment at 1204 °C (2200 °F) had a very large grain size, as might be expected. The microstructure appears blocky rather than a stringer type, however, which may indicate that grain size does not always dictate the grain morphology. It was also noted that the grain boundaries

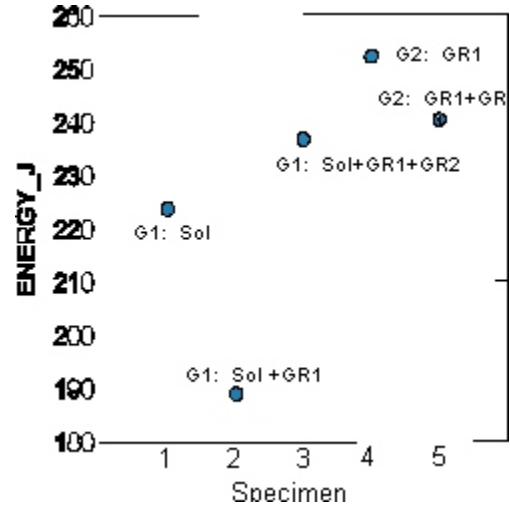


Figure 13. Specimens tested at various stages of the heat treatment are identified by specimen numbers assigned in Table 2. The group (G1 or G2), solution treatment (sol), and grain refinement steps (GR1 and GR2) for the specimens are also indicated.

etch unevenly, and this may indicate that precipitates or slight chemical inhomogeneities are present at the boundaries even for the hardest quenched specimens.

The group 1 specimen that was solution treated, then re-heated slowly to 815 °C (1500 °F) for 10 min had a predominantly stringy martensitic structure (**Figure 15**). The group 1 specimen (**Figures 16 and 17**) that was solution annealed and re-heated twice for grain refinement had a mixture of blocky and stringer-type structures. More importantly, the grain size is clearly refined compared to that for the as-solution-treated structure (**Figure 14**). This specimen had the highest toughness.

The group 2 specimens (**Figures 18-19**), which were not solution treated, show slight differences in structure from one another. The specimen that received only one grain-refinement step, **Figure 18**, has reverted austenite at prior austenite grain boundaries and on preferred planes within the grains (as does the as-received T-200 bar stock). This specimen had the highest energy for the heat-treatment conditions considered here. The specimen that received both grain-refinement treatments (**Figure 19**) has a slightly larger grain size, and less reverted austenite is apparent. Both specimens retained a reasonably small grain size (probably less than 25 μm). The slightly higher toughness of the specimen in **Figure 18**, may reflect the smaller grain size and/or the presence of more reverted austenite in the structure.

Comparing the group 1 and 2 specimens, grain-refinement treatments following the solution-treatment were effective in reducing the very large grain size of the as-solution-treated specimens. The large grain in the center of the solution treated specimen shown in **Figure 14** is about 500 μm in diameter, compared with grain diameters on the order of 10 to 20 μm in the nonsolution-treated group 2 specimens (**Figures 18 - 19**). It is not clear whether any grain refinement occurred in the group 2 specimens. These specimens have grain sizes similar to the as-received T-200 material.

The solution treatment did not result in a change to the large indigenous Ti(N,C) inclusion content or size distribution, as might be expected (the melting point of these inclusions is over 2900 °C). Measurements on group 1 and group 3 specimens (400 fields per sample) show the Ti-rich inclusions to favor cube-like morphologies with an average size of about 11 μm (cube edge). The average number of Ti(C,N) inclusions per millimeter squared was estimated to be about 10. There were differences in the amounts of smaller indigenous inclusions in the samples. The as-received sample had a significantly higher number of inclusions with diameters in the range of about 2 to 30 μm. Detailed evaluations of these smaller inclusions (which may also include small islands of retained austenite) were not done, however, so no data on these inclusions are available (the inclusion counts were done at too low a magnification to yield accurate information on these smaller inclusions).

Since the solution treatment does not result in a beneficial modification to the large Ti-rich inclusions, and the as-received material was not found to be embrittled, it appears that there is little need to include a solution treatment in the processing of this material, unless it results in lower scatter to the specimens following the final annealing treatments.

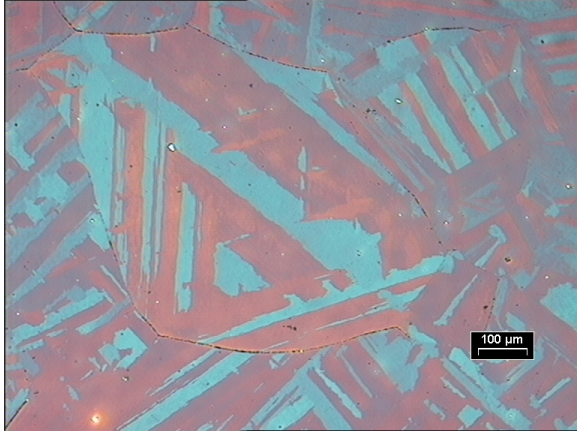


Figure 14. Specimen G1-1

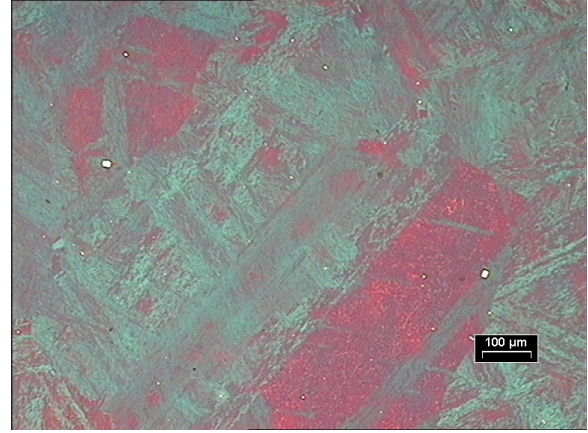


Figure 15. Specimen G1-2

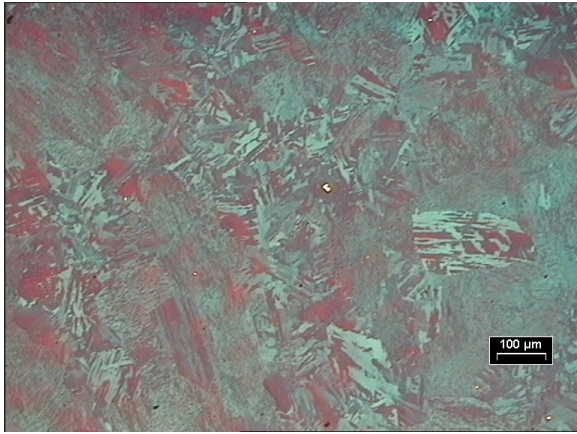


Figure 16. Specimen G1-3

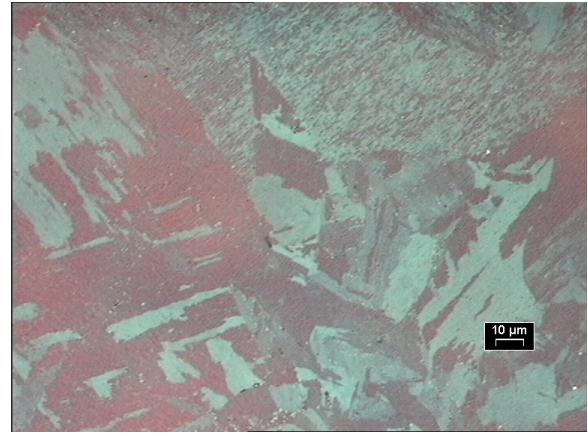


Figure 17. Specimen G1-3



Figure 18. Specimen G2-1



Figure 19. Specimen G2-2

Final Annealing treatments (1 through 4)

The microstructures of the specimens after the final annealing treatments showed that the group 2 and group 3 specimens had smaller grain size than the group 1 specimens. In **Figure 20**, for example, the grain size of the group 1 specimen is larger than that of the group 3 specimens shown in **Figures 21 and 22**. The group 1 specimens, the only specimen group that was solution-annealed, had some grains as large as 100 μm , and many grain diameters were assumed to be between 20 and 40 μm .

The group 2 and group 3 specimens had similar grain sizes. However, those specimens that were annealed at the lower temperature (**Figure 21**) generally had a smaller grain size (typical sizes range between 4 and 20 μm in **Figure 21**) than those annealed at higher temperature (typical sizes range between 15 to 30 μm). So, some grain growth was associated with the final annealing treatments, particularly for the higher-temperature anneals (900 $^{\circ}\text{C}$, 1650 $^{\circ}\text{F}$), but grain sizes remained reasonable for all of the treatments.

The impact-test results are summarized in **Figure 23**. The results of anneal 1 (1525 $^{\circ}\text{F}$, 2 h, 5 bar helium quench) showed that a slightly higher absorbed energy (157 ft-lbs) was attained for the group 1 specimens, which were solution-annealed. The group 3 specimens, however, had lower scatter in absorbed energy than the group 1 or group 2 specimens. So the particular solution and grain refinement treatments used here for the Group 1 and 2 specimens did not reduce the scatter in impact energy over that found for the as-received and annealed specimens.

The results of anneal 2 (1525 $^{\circ}\text{F}$, 2 h, 1 bar nitrogen quench) again show that the group 1 specimens have slightly higher toughness (153 ft-lbs) than the group 2 or group 3 specimens (147 and 149 ft-lbs). However, the slower quench used for this annealing step resulted in higher scatter

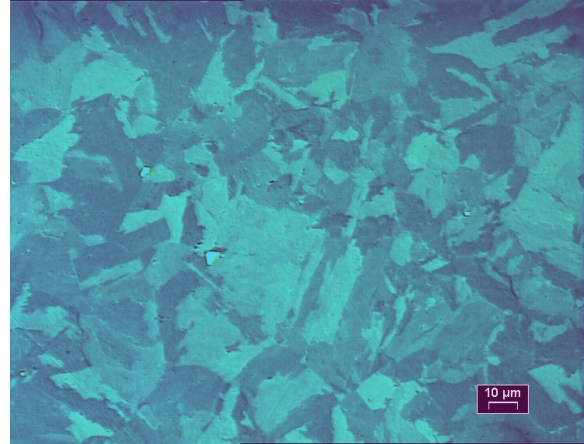


Figure 20. A group 1 specimen, with a high-temperature anneal, specimen # 391. Bar equal to 10 μm .

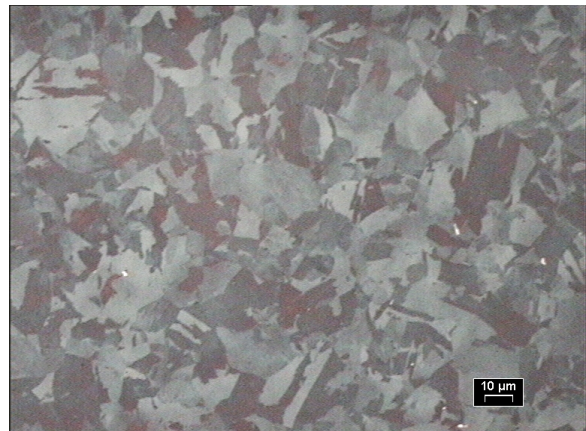


Figure 21. A group 3 specimen, with a low-temperature anneal, specimen # 2.

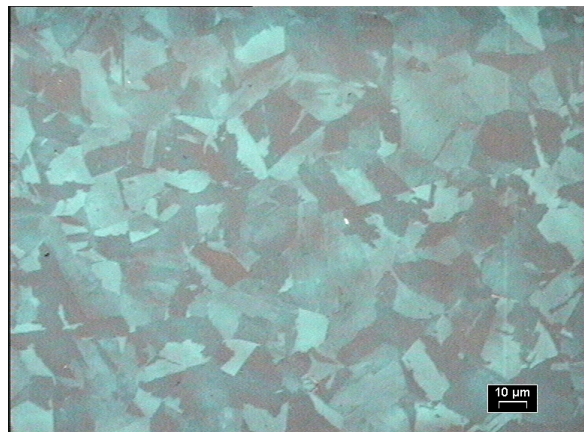


Figure 22. A group 3 specimen with high-temperature anneal (#36)

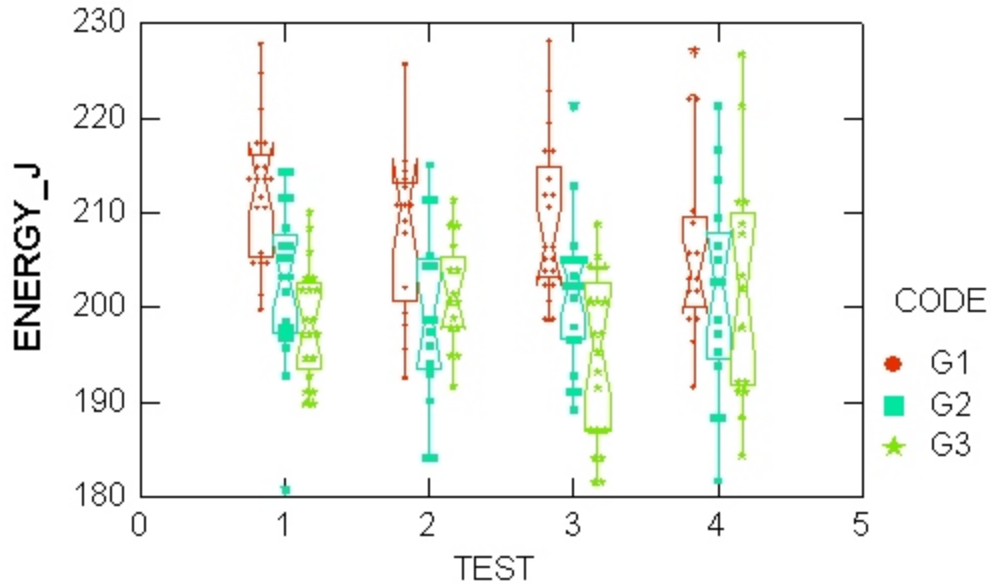


Figure 23. Box plot of the data for the final annealing treatments.

(coefficient of variation) for groups 1 and 2 (0.042 and 0.047), compared with the results for anneal 1 (0.035 and 0.040). The scatter for the group 3 specimens is the exception here, where similar low levels of scatter (0.03) were found to be independent of cooling rate.

The anneal 3 (1650 °F, 2 h, 5 bar helium quench) produced data of impact energy similar to that for the anneal 1 and 2 treatments: 154, 149, and 144 ft-lbs for groups 1, 2, and 3, respectively. The scatter in absorbed energy for the group 1 and 2 specimens (0.039 and 0.039) was similar to previous results, but the scatter for the group 3 specimens increased (0.045).

The data for the anneal 4 specimens (1650 °F, 2 h, 1 bar nitrogen quench) showed absorbed energy levels similar to all the previous data, but had consistently higher scatter in absorbed energy: The coefficients of variation for group 1, 2, and 3 were 0.049, 0.055, and 0.062, respectively. Again, the slower quench rate (used to simulate an air cool for this annealing treatment) resulted in higher scatter for the specimens.

Summary

Results of this study and the initial studies on this T-200 material have provided useful information for the production and quality control of the super-high-energy specimens. A summary of our understanding for the new T-200 material is as follows:

- The T-200 material is relatively homogeneous.
- The T-200 material can be used to produce impact verification specimen having energies of near 200 J.
- A minimum temperature 815 °C (1500 °F) is suggested for annealing treatments.
- A maximum annealing temperature of about 870 °C (1600 °F) is suggested.
- Significant grain growth occurs at temperatures above 900 °C (1700 °F, for 1 h).

- Grain refinement is possible if grain growth occurs during heat treatment.
- A small, more or less equiaxed grain morphology (less than 30 μm) with well defined grain boundaries is desirable.
- Increasing the amount of reverted austenite in the microstructure appears to increase the toughness of the material (but the effect on variation in the absorbed energy was not evaluated)
- The variation in the absorbed energy is likely reduced by quenching the material rather than allowing it to cool more slowly.
- The variation in the absorbed energy was not clearly reduced by solution treatments or by grain refinement treatments.

CODE	NUM	ANNEAL	Anneal code	ENERGY (ft-lbf)	Energy (J)	HARD (HRC)
G1	1	SOL	0	165	224	25
G1	2	SOL_GR1	0	139	189.0	30
G1	3	SOL_GR1_GR2	0	175	237	28
G2	1	GR1_ONLY	0	186	252	28
G2	2	GR1_GR2	0	177	240	27
G1	4	GR1_5BAR	1	158	214	30
G1	5	GR1_5BAR	1	158	214	30
G1	6	GR1_5BAR	1	158	215	30
G1	7	GR1_5BAR	1	147	200	30
G1	8	GR1_5BAR	1	160	217	30
G1	9	GR1_5BAR	1	151	205	30
G1	10	GR1_5BAR	1	155	211	30
G1	11	GR1_5BAR	1	166	225	30
G1	12	GR1_5BAR	1	158	214	30
G1	13	GR1_5BAR	1	152	206	30
G1	14	GR1_5BAR	1	160	218	
G1	15	GR1_5BAR	1	148	201	
G1	16	GR1_5BAR	1	156	212	
G1	17	GR1_5BAR	1	151	204	
G1	18	GR1_5BAR	1	168	228	
G1	19	GR1_5BAR	1	151	205	
G1	20	GR1_5BAR	1	159	215	
G1	21	GR1_5BAR	1	155	210	
G1	22	GR1_5BAR	1	163	221	
G1	23	GR1_5BAR	1	158	214	
G2	3	GR1_5BAR	1	152	206	31
G2	4	GR1_5BAR	1	152	206	31
G2	5	GR1_5BAR	1	146	198	31
G2	6	GR1_5BAR	1	133	181	31
G2	7	GR1_5BAR	1	146	198	31
G2	8	GR1_5BAR	1	151	205	31
G2	9	GR1_5BAR	1	150	203	31
G2	10	GR1_5BAR	1	156	212	31
G2	11	GR1_5BAR	1	149	202	31
G2	12	GR1_5BAR	1	146	198	31
G2	13	GR1_5BAR	1	153	207	
G2	14	GR1_5BAR	1	145	197	
G2	15	GR1_5BAR	1	158	214	
G2	16	GR1_5BAR	1	144	196	
G2	17	GR1_5BAR	1	156	211	
G2	18	GR1_5BAR	1	154	208	
G2	19	GR1_5BAR	1	142	193	
G2	20	GR1_5BAR	1	145	197	
G2	21	GR1_5BAR	1	158	214	
G2	22	GR1_5BAR	1	150	203	
G3	1	GR1_5BAR	1	140	190	31
G3	2	GR1_5BAR	1	143	194	31
G3	3	GR1_5BAR	1	141	191	31
G3	4	GR1_5BAR	1	142	193	31
G3	5	GR1_5BAR	1	150	203	31
G3	6	GR1_5BAR	1	146	198	31
G3	7	GR1_5BAR	1	149	202	31
G3	8	GR1_5BAR	1	141	191	31

CODE	NUM	ANNEAL	Anneal code	ENERGY (ft-lbf)	Energy (J)	HARD (HRC)
G3	9	GR1_5BAR	1	150	203	31
G3	10	GR1_5BAR	1	154	208	31
G3	11	GR1_5BAR	1	149	202	
G3	12	GR1_5BAR	1	140	190	
G3	13	GR1_5BAR	1	155	210	
G3	14	GR1_5BAR	1	149	202	
G3	15	GR1_5BAR	1	147	199	
G3	16	GR1_5BAR	1	152	206	
G3	17	GR1_5BAR	1	146	198	
G3	18	GR1_5BAR	1	145	197	
G3	19	GR1_5BAR	1	144	195	
G3	20	GR1_5BAR	1	145	197	
G1	24	GR1_1BAR	2	144	195	30
G1	25	GR1_1BAR	2	149	202	30
G1	26	GR1_1BAR	2	155	211	30
G1	27	GR1_1BAR	2	153	208	30
G1	28	GR1_1BAR	2	142	193	30
G1	29	GR1_1BAR	2	157	213	31
G1	30	GR1_1BAR	2	159	215	30
G1	31	GR1_1BAR	2	166	226	30
G1	32	GR1_1BAR	2	155	211	30
G1	33	GR1_1BAR	2	156	211	30
G1	34	GR1_1BAR	2	158	214	30
G1	35	GR1_1BAR	2	158	214	30
G1	36	GR1_1BAR	2	146	198	30
G1	37	GR1_1BAR	2	154	209	30
G1	38	GR1_1BAR	2	147	199	30
G2	23	GR1_1BAR	2	156	211	31
G2	24	GR1_1BAR	2	159	215	31
G2	25	GR1_1BAR	2	144	196	31
G2	26	GR1_1BAR	2	143	194	31
G2	27	GR1_1BAR	2	142	193	31
G2	28	GR1_1BAR	2	146	197	31
G2	29	GR1_1BAR	2	136	184	31
G2	30	GR1_1BAR	2	146	198	31
G2	31	GR1_1BAR	2	140	190	31
G2	32	GR1_1BAR	2	156	212	31
G2	33	GR1_1BAR	2	152	206	
G2	34	GR1_1BAR	2	151	204	
G2	35	GR1_1BAR	2	147	199	
G2	36	GR1_1BAR	2	136	184	
G2	37	GR1_1BAR	2	151	205	
G3	21	GR1_1BAR	2	148	200	31
G3	22	GR1_1BAR	2	151	204	31
G3	23	GR1_1BAR	2	146	198	31
G3	24	GR1_1BAR	2	156	211	31
G3	25	GR1_1BAR	2	147	199	31
G3	26	GR1_1BAR	2	152	207	31
G3	27	GR1_1BAR	2	150	204	31
G3	28	GR1_1BAR	2	144	195	31
G3	29	GR1_1BAR	2	148	201	31
G3	30	GR1_1BAR	2	141	192	31
G3	31	GR1_1BAR	2	144	195	

CODE	NUM	ANNEAL	Anneal code	ENERGY (ft-lbf)	Energy (J)	HARD (HRC)
G3	32	GR1_1BAR	2	154	209	
G3	33	GR1_1BAR	2	149	201	
G3	34	GR1_1BAR	2	154	208	
G3	35	GR1_1BAR	2	146	198	
G1	39	GR2_5BAR	3	160	217	30
G1	40	GR2_5BAR	3	168	228	30
G1	41	GR2_5BAR	3	147	199	30
G1	42	GR2_5BAR	3	150	204	30
G1	43	GR2_5BAR	3	148	201	29
G1	44	GR2_5BAR	3	156	212	30
G1	45	GR2_5BAR	3	153	207	30
G1	46	GR2_5BAR	3	151	204	30
G1	47	GR2_5BAR	3	155	210	30
G1	48	GR2_5BAR	3	147	199	30
G1	49	GR2_5BAR	3	152	206	
G1	50	GR2_5BAR	3	150	203	
G1	51	GR2_5BAR	3	164	223	
G1	52	GR2_5BAR	3	149	202	
G1	53	GR2_5BAR	3	151	205	
G1	54	GR2_5BAR	3	162	219	
G1	55	GR2_5BAR	3	160	216	
G1	56	GR2_5BAR	3	157	212	
G1	57	GR2_5BAR	3	158	214	
G1	58	GR2_5BAR	3	152	205	
G2	38	GR2_5BAR	3	140	189	30
G2	39	GR2_5BAR	3	141	192	31
G2	40	GR2_5BAR	3	151	205	31
G2	41	GR2_5BAR	3	148	201	30
G2	42	GR2_5BAR	3	151	205	31
G2	43	GR2_5BAR	3	151	205	31
G2	44	GR2_5BAR	3	145	197	31
G2	45	GR2_5BAR	3	150	203	31
G2	46	GR2_5BAR	3	149	202	30
G2	47	GR2_5BAR	3	145	197	31
G2	48	GR2_5BAR	3	157	213	
G2	49	GR2_5BAR	3	146	198	
G2	50	GR2_5BAR	3	152	205	
G2	51	GR2_5BAR	3	152	206	
G2	52	GR2_5BAR	3	141	191	
G2	53	GR2_5BAR	3	163	221	
G2	54	GR2_5BAR	3		0	
G2	55	GR2_5BAR	3	149	202	
G2	56	GR2_5BAR	3	142	193	
G2	57	GR2_5BAR	3	150	203	
G3	36	GR2_5BAR	3	151	204	31
G3	37	GR2_5BAR	3	138	187	31
G3	38	GR2_5BAR	3	138	187	31
G3	39	GR2_5BAR	3	145	197	31
G3	40	GR2_5BAR	3	136	184	31
G3	41	GR2_5BAR	3	151	204	31
G3	42	GR2_5BAR	3	138	187	31
G3	43	GR2_5BAR	3	144	195	31
G3	44	GR2_5BAR	3	141	192	31

CODE	NUM	ANNEAL	Anneal code	ENERGY (ft-lbf)	Energy (J)	HARD (HRC)
G3	45	GR2_5BAR	3	151	205	31
G3	46	GR2_5BAR	3	134	182	
G3	47	GR2_5BAR	3	148	201	
G3	48	GR2_5BAR	3	154	209	
G3	49	GR2_5BAR	3	148	201	
G3	50	GR2_5BAR	3	136	184	
G3	51	GR2_5BAR	3	146	198	
G3	52	GR2_5BAR	3	143	193	
G3	53	GR2_5BAR	3	134	181	
G3	54	GR2_5BAR	3	152	205	
G3	55	GR2_5BAR	3	148	201	
G1	59	GR2_1BAR	4	149	201	30
G1	60	GR2_1BAR	4	149	202	30
G1	61	GR2_1BAR	4	147	199	30
G1	62	GR2_1BAR	4	152	205	30
G1	63	GR2_1BAR	4	147	199	30
G1	64	GR2_1BAR	4	152	206	30
G1	65	GR2_1BAR	4	150	203	30
G1	66	GR2_1BAR	4	150	203	30
G1	67	GR2_1BAR	4	141	192	30
G1	68	GR2_1BAR	4	154	209	30
G1	69	GR2_1BAR	4	168	227	
G1	70	GR2_1BAR	4	164	222	
G1	71	GR2_1BAR	4	145	196	
G1	72	GR2_1BAR	4	164	222	
G1	73	GR2_1BAR	4	155	210	
G2	58	GR2_1BAR	4	143	194	
G2	59	GR2_1BAR	4	151	205	
G2	60	GR2_1BAR	4	139	189	
G2	61	GR2_1BAR	4	139	188	
G2	62	GR2_1BAR	4	158	214	
G2	63	GR2_1BAR	4	144	195	
G2	64	GR2_1BAR	4	150	203	
G2	65	GR2_1BAR	4	147	199	
G2	66	GR2_1BAR	4	163	221	
G2	67	GR2_1BAR	4	134	182	
G2	68	GR2_1BAR	4	155	209	
G2	69	GR2_1BAR	4	150	203	
G2	70	GR2_1BAR	4	146	197	
G2	71	GR2_1BAR	4	152	206	
G2	72	GR2_1BAR	4	160	217	
G3	56	GR2_1BAR	4	153	208	
G3	57	GR2_1BAR	4	142	193	
G3	58	GR2_1BAR	4	150	203	
G3	59	GR2_1BAR	4	136	184	
G3	60	GR2_1BAR	4	141	191	
G3	61	GR2_1BAR	4	149	202	
G3	62	GR2_1BAR	4	142	192	
G3	63	GR2_1BAR	4	154	209	
G3	64	GR2_1BAR	4	156	211	
G3	65	GR2_1BAR	4	146	198	
G3	66	GR2_1BAR	4	167	227	
G3	67	GR2_1BAR	4	163	221	

CODE	NUM	ANNEAL	Anneal code	ENERGY (ft-lbf)	Energy (J)	HARD (HRC)
G3	68	GR2_1BAR	4	139	188	
G3	69	GR2_1BAR	4	141	192	
G3	70	GR2_1BAR	4	156	212	

Anneal code	Group CODE	STATISTIC	ENERGY J (ft-lbf)	HARD (HRC)
0	G1	N of cases	1	1
0	G1	Mean	234 (165)	25
0	G1	N of cases	1	1
0	G1	Mean	188 (139)	30
0	G1	N of cases	1	1
0	G1	Mean	237 (175)	28
0	G2	N of cases	1	1
0	G2	Mean	252 (186)	28
0	G2	N of cases	1	1
0	G2	Mean	240 (177)	27
1	G1	N of cases	20	10
1	G1	Minimum	199 (147)	30
1	G1	Maximum	228 (168)	30
1	G1	Range	28 (21)	1
1	G1	Median	214 (158)	30
1	G1	Mean	213 (157)	30
1	G1	Standard Dev	7 (5)	0
1	G1	C.V.	0	0
1	G2	N of cases	20	10
1	G2	Minimum	180 (133)	31
1	G2	Maximum	214 (158)	31
1	G2	Range	34 (25)	0
1	G2	Median	203 (150)	31
1	G2	Mean	202 (149)	31
1	G2	Standard Dev	8 (6)	0
1	G2	C.V.	0	0
1	G3	N of cases	20	10
1	G3	Minimum	190 (140)	31
1	G3	Maximum	210 (155)	31
1	G3	Range	20 (15)	0
1	G3	Median	198 (146)	31
1	G3	Mean	198 (146)	31
1	G3	Standard Dev	5 (4)	0
1	G3	C.V.	0	0
2	G1	N of cases	15	15
2	G1	Minimum	193 (142)	30
2	G1	Maximum	225 (166)	31
2	G1	Range	32 (24)	1
2	G1	Median	210 (155)	30
2	G1	Mean	207 (153)	30
2	G1	Standard Dev	10 (7)	0
2	G1	C.V.	0	0
2	G2	N of cases	15	10
2	G2	Minimum	184 (136)	31
2	G2	Maximum	216 (159)	31
2	G2	Range	32 (23)	1
2	G2	Median	198 (146)	31
2	G2	Mean	199 (147)	31
2	G2	Standard Dev	10 (7)	0
2	G2	C.V.	0	0
2	G3	N of cases	15	10
2	G3	Minimum	191 (141)	31
2	G3	Maximum	212 (156)	31
2	G3	Range	21 (15)	0

Anneal code	Group CODE	STATISTIC	ENERGY J (ft-lbf)	HARD (HRC)
2	G3	Median	201 (148)	31
2	G3	Mean	202 (149)	31
2	G3	Standard Dev	5 (4)	0
2	G3	C.V.	0	0
3	G1	N of cases	20	10
3	G1	Minimum	199 (147)	29
3	G1	Maximum	228 (168)	30
3	G1	Range	29 (22)	1
3	G1	Median	206 (152)	30
3	G1	Mean	209 (154)	30
3	G1	Standard Dev	8 (6)	0
3	G1	C.V.	0	0
3	G2	N of cases	19	10
3	G2	Minimum	190 (140)	30
3	G2	Maximum	221 (163)	31
3	G2	Range	33 (24)	1
3	G2	Median	202 (149)	31
3	G2	Mean	202 (149)	31
3	G2	Standard Dev	8 (6)	0
3	G2	C.V.	0	0
3	G3	N of cases	20	10
3	G3	Minimum	182 (134)	31
3	G3	Maximum	209 (154)	31
3	G3	Range	27 (20)	1
3	G3	Median	197 (145)	31
3	G3	Mean	195 (144)	31
3	G3	Standard Dev	8 (6)	0
3	G3	C.V.	0	0
4	G1	N of cases	15	10
4	G1	Minimum	191 (141)	30
4	G1	Maximum	228 (168)	30
4	G1	Range	35 (26)	0
4	G1	Median	203 (150)	30
4	G1	Mean	206 (152)	30
4	G1	Standard Dev	11 (8)	0
4	G1	C.V.	0	0
4	G2	N of cases	15	0
4	G2	Minimum	182 (134)	
4	G2	Maximum	221 (163)	
4	G2	Range	39 (29)	
4	G2	Median	203 (150)	
4	G2	Mean	202 (149)	
4	G2	Standard Dev	11 (8)	
4	G2	C.V.	0	
4	G3	N of cases	15	0
4	G3	Minimum	184 (136)	
4	G3	Maximum	226 (167)	
4	G3	Range	42 (31)	
4	G3	Median	202 (149)	
4	G3	Mean	202 (149)	
4	G3	Standard Dev	12 (9)	
4	G3	C.V.	0	

1. Saul, G.; Roberson, J.A.; Adair, A.M.; The Effects of Thermal Treatment on the Grain Size and Mechanical Properties of 18 Ni Maraging Steels, *Met. Trans.*, Vol. 1, February 1970, pp. 383-387.
2. Viswanathan, U.K.; Kutty, T.R.G.; Ganguly, C.; Dilatometric Technique for Evaluation of the Kinetics of Solid-State Transformation of Maraging Steel, *Met. Trans.* Vol. 24, December 1993, pp. 2653-2656.
3. Sarma, D.S.; Sinha, P.P.; Structure-Property Correlations in a Co-free Maraging Steel, *Trans. Indian Inst. Met.*, Vol. 49, No.3, June 1996, pp. 163-169.
4. Viswanathan, U.K.; Kishore, R.; Asundi, M.K.; Effect of Thermal Cycling on the Mechanical Properties of 350-Grade Maraging Steel, *Metallurgical and Material Transactions A*, Vol. 27A, March 1996, pp. 757-761.
5. Sinha, P.P.; Tharian, T.T.; Sivakumar, D.; Sarma, D.S.; Effects of Solution Temperatures on Microstructure, Tensile, and Fracture Properties of Co-free 18 Ni Maraging Steel, *Steel Research*, 65, Vol. No. 11, 1994, pp. 494-499.
6. Sinha, P.P.; Sreekumar, K.; Nargarajan, K.V.; Grain Growth in 18 Ni Co-free Maraging Steel, *Trans. Indian Inst. Met.*, Vol. 52, No. 2-3, April-June 1999, pp. 119-124.
7. Tewari, S.; Mazumder, I.S.; Batra, G.K.; Dey, Banerjee, S.; Precipitation in 18 Ni Maraging Steel of Grade 350, *Acta mater*, 48, 2000, pp. 1187-1200.
8. Sinha, K.; Tharian, T.; Sreekumar, K.; Nargarajan, K.V.; Sarma, D.S.; Effect of Aging on Microstructure and Mechanical Properties of Cobalt Free 18Ni250 Maraging Steel, *Materials Science and Technology*, January 1998, Vol 14, pp. 1-9.
9. Sinha, D.; Sivakumar, K.T.; Tharian, K.V.; Nargarajan, and D.S. Sarma, Thermal Embrittlement in 18Ni Cobalt Free and 18Ni-8Co-5Mo Maraging Steels, *Material Science and Technology*, November 1996, Vol 12, pp. 945-954.